A Polarimetric Generalized Likelihood Ratio Detector for Scattering Centers in K-distributed Clutter

R. L. Dilsavor and R. L. Moses
Department of Electrical Engineering
The Ohio State University
Columbus, OH, 43210

Abstract

This paper considers the problem of detecting targets in a forest using a wideband, polarimetric synthetic aperture radar (SAR). First, we find that SAR forest measurements are well-modeled by the K-distribution. Second, we display histograms of the Huynen parameters of SAR data in order to describe clutter behavior. We then focus on optimal techniques for exploiting polarimetric information to detect point targets. We assume that the point target has an unknown amplitude, unknown orientation about the radar line-of-site, and unknown absolute phase. This assumption leads to a composite-hypothesis detection problem with nuisance parameters. We develop a generalized likelihood ratio test to accomodate the unknowns and demonstrate a bounded two-dimensional search for finding their maximum likelihood estimates.

1 Introduction

This paper considers the problem of detecting targets of interest in a clutter-filled environment by processing radar data which is fully-polarimetric and is collected over an ultra-wide bandwidth by a low-frequency SAR. We are interested in techniques which combine information across polarization for the purpose of detecting point targets in forest clutter. We assume that the frequency diverse measurements are used to obtain high resolution, complex in-phase and quadrature (IQ), time-domain pulse responses at each position along the synthetic aperture. Thus, we have three complex responses (HH, HV, and VV) at each aperture position. These angle diverse responses are combined using a SAR or tomographic imaging technique to create two-dimensional HH, HV, and VV images of the observed area [1].

In many problems of practical interest, the detection is complicated by a target which is incompletely specified. We make the realistic assumption that the target amplitude, orientation about the line-of-sight, and absolute phase may be unknown. We design a generalized likelihood ratio test (GLRT) for detecting a target with these unknowns [2, 3].

In order to design the GLRT, we need models for target and clutter scattering. In our application, the clutter consists of scattering from a forest and the targets of interest are canonical scattering centers. The full-polarization scattering characteristics of many canonical point targets such as dipoles, flat plates, and dihedrals are well-documented [4, 5]. In our application, we require clutter pixel statistics at 1.0×1.0 ft resolution in the frequency range 0.2 - 1.5 GHz. These clutter statistics are not widely available in the literature. Hence, this research begins with a statistical analysis of forest clutter at the resolution and frequency range given above. We then use these statistical results to develop a GLRT-based detection algorithm.

The next section briefly describes the SAR system and forest clutter environment. Section 3 presents the polarimetric mean and covariance of the forest clutter measurements . Section 4 compares the ability of the Gaussian and K-distributions to model forest clutter scattering. Section 5 provides histograms of the Huynen parameters of the SAR images. Section 6 presents a polarimetric GLRT approach to scattering center detection. Section 7 presents some preliminary results in the implementation and performance of the polarimetric GLRT. The final section presents our conclusions.

2 SAR System Description

Forest clutter data was measured by a proof-of-concept linear aperture SAR. The SAR has an aperture length of 120 ft while the aperture spacing between successive measurements is 4 inches giving a total of 361 measured signals. The aperture is approximately 95 ft above ground level and the radar views the forest at a declination angle of 8°. The forest clut-

ter image area extends the length of the aperture (120 ft), has a downrange dimension of 50 ft, and begins at a range of 147 ft. Figure 1 shows the radar geometry. This central Ohio site consists of gently rolling, glaciated upland that supports a mixed deciduous forest dominated by northern red oak, black cherry, and hickory. Tree sizes range primarily from 4-12 inches dbh (diameter at breast height) with relatively few larger trees exceeding 20 inches dbh. The site is fully-forested with a basal area of 106 sq ft/acre in trees exceeding 2 inches dbh.

Measurements were made in the ultra-wide, low frequency range 0.22 - 1.56 GHz. These frequency measurements were used to synthesize the complex IQ time domain pulse responses. Complex HH, HV, and VV images were formed using a modified convolution backprojection algorithm [1] applied to the pulse responses. The downrange resolution of the images is 8.9 inches and the crossrange resolution at the maximum frequency of 1.56 GHz is 10.4 inches.

3 Clutter Mean and Covariance

Let X_{Ci} be the complex vector containing samples of the HH, HV and VV images at the ith pixel and let X_{Ri} be the real 6-vector containing the real and imaginary parts of the elements of X_{Ci};

$$X_{Ci} = [\ HH_i \quad HV_i \quad VV_i\ ]^T \qquad (1)$$

$$X_{Ri} = [\ Re(HH_i) \quad Im(HH_i) \quad \cdots\ ]^T. \qquad (2)$$

The sample mean and covariance of the X_{Ci} and X_{Ri} were computed as simple block averages over the number of pixels. The experimental results are presented in polar format with angle in degrees:

$$\overline{X_C} =$$
$$[\ 0.675\angle-144.9 \quad 0.158\angle-118.1 \quad 0.360\angle-143.4\ ]^T \qquad (3)$$
$$COV(X_C) =$$
$$\begin{bmatrix} 0.651\angle 0 & 0.0246\angle-132.5 & 0.0722\angle-82.3 \\ 0.0246\angle132.5 & 0.1196\angle 0 & 0.0074\angle-120.5 \\ 0.0722\angle82.3 & 0.0074\angle120.5 & 0.2371\angle 0 \end{bmatrix} \qquad (4)$$
$$\overline{X_R} =$$
$$[\ -0.552 \quad -0.388 \quad -0.075 \quad -0.140 \quad -0.289 \quad -0.215\ ]^T \qquad (5)$$
$$COV(X_R) =$$
$$\begin{bmatrix} 0.3308 & 0.0110 & -0.0101 & 0.0076 & 0.0108 & 0.0393 \\ 0.0110 & 0.3203 & -0.0106 & -0.0065 & -0.0323 & -0.0011 \\ -0.0101 & -0.0106 & 0.0586 & -0.0028 & 0.0016 & 0.0025 \\ 0.0076 & -0.0065 & -0.0028 & 0.0610 & -0.0039 & -0.0053 \\ 0.0108 & -0.0323 & 0.0016 & -0.0039 & 0.1066 & -0.0021 \\ 0.0393 & -0.0011 & 0.0025 & -0.0053 & -0.0021 & 0.1305 \end{bmatrix} \qquad (6)$$

Notice from (3)–(6) that the pixel values are largely zero mean and that for any polarization the real and imaginary parts of a pixel value are largely uncorrelated. These observations agree with findings in [6]. Our measurements show a weaker VV response relative to HH and a smaller correlation coefficient between HH and VV than do those of Novak [7]. (In [7] the radar has a resolution similar to ours but operates

at a much higher frequency of 33GHz.) We expect that the difference in HH-VV correlation is due to the small declination angle and lower frequency range of our radar.

4 Gaussian and K-Distributions

Several families of distributions have been used to model clutter scattering. Gaussian statistics have been assumed in many instances [6, p. 237], [8]. Product models such as Weibull, lognormal, and the K-distribution have been found to more accurately model "heavy-tail" forest clutter distributions [6, 7], [9]–[11]. We compare the ability of the Gaussian and K-distributions to adequately model forest clutter scattering at our low frequencies and wide bandwidth.

The real Gaussian distributed vector X with mean m_x and covariance Σ_x is denoted $X : N(m_x, \Sigma_x)$. Similarly, the real K-distributed vector Y is denoted $Y : K(\alpha, m_y, \Sigma_y)$ where α is the shape-adjusting parameter for the K-distribution. In our work, we use the one-parameter, non-zero mean version of the K-distribution that is derived using the homodyned approach [6].

Figure 2 shows the Gaussian and K-distributed densities overlayed on the histogram of the real part of HH. To generate the analytical pdf curves, we assume that the clutter is zero-mean ($m_x = m_y = 0$), as supported by experimental evidence. The clutter covariance is given by (6). Using the technique of [6, pp. 242, 248] we estimated the parameter α to be $\alpha = 2.56$. Qualitatively, we see that the narrower central lobe of the K-distribution more accurately models the histogram of the clutter scattering. The plots for HV and VV polarizations are similar.

5 Clutter Huynen Parameters

Huynen [4] expresses a general scattering matrix in terms of several geometrically relevant descriptors

$$S = me^{j2\rho}U^*(\psi,\tau,\nu)\begin{bmatrix} 1 & 0 \\ 0 & \tan^2\gamma \end{bmatrix} U^H(\psi,\tau,\nu)$$

where $U(\cdot,\cdot,\cdot)$ is unitary. The positive-valued descriptor m is the radar target magnitude. $\psi \in [0,\pi]$ and $\tau \in [-45°, 45°]$ are the tilt angle and ellipticity, respectively, of the polarization state that leads to maximum power received from the target. The angle $\nu \in [-45°, 45°]$ is the target skip angle and is related to the number of bounces of the reflected signal. The angle $\gamma \in [0°, 45°]$ is called the characteristic angle of the target and relates the strengths of the maximum and minimum responses of the target to an incident wave of varying polarization. The absolute

phase $\rho \in [-90°, 90°]$ of the target depends upon the target range.

Figure 3 shows histograms of the Huynen parameters of the clutter images. Let p_m denote the incident polarization state which causes the scattered signal from a clutter pixel to have maximum amplitude. Then the target amplitude m is that maximum amplitude. The histogram of m is similar to a Rayleigh distribution as would be expected for the maximum eigenvalue of a nearly Gaussian scattering matrix S. If the polarization state $p_m^\perp$ that is orthogonal to p_m is incident on the clutter pixel, then the scattered signal would have amplitude $m \tan^2 \gamma$ where γ is the characteristic angle. In other words, $\tan^2 \gamma$ gives the ratio of the minimum to maximum eigenvalues of S. We find that this ratio is $\overline{\tan^2 \gamma} = 0.39$ on the average with a standard deviation $std(\tan^2 \gamma) = 0.20$. The tilt angle ψ of polarization state p_m is concentrated around $0°$, or horizontal. The histogram for the ellipticity τ of polarization state p_m peaks at $0°$ (ie. linear) and tapers down to zero at $\pm45°$ (ie. right and left circular). The skip angle ν has a nearly uniform distribution over its range with a slight preference towards $-15°$. Hence, the clutter has a blending of odd and even bounce mechanisms. The absolute phase ρ is uniformly distributed over its range, as expected.

6 Polarimetric GLRT Approach

Our approach to detecting canonical scattering centers in forest clutter is motivated by the assumption that a target scattering center is completely known except for its amplitude m, absolute phase ρ, and orientation ψ about the line-of-sight. We explicitly denote these unknowns in our model of the received signal

$$H_0 : \quad X_R = \quad C$$
$$H_1 : \quad X_R = \quad C + m \cdot R(\rho)P(\psi)T_n$$

where we use the real vector representation of the data as in (2). In this model, T_n is a nominal target which is defined as having amplitude $m \overset{\triangle}{=} 1$, phase $\rho \overset{\triangle}{=} 0$, and orientation about the line-of-sight $\psi \overset{\triangle}{=} 0$. After premultiplying T_n by the matrices $P(\psi)$ and $R(\rho)$ and the scalar m, the resulting target contribution has amplitude m, phase ρ, and orientation ψ. The form of $R(\cdot)$ and $P(\cdot)$ are found easily and are not presented here. In addition, the clutter is taken to be distributed as $K(\alpha, 0, \Sigma)$.

If m, ρ, and ψ were known then this problem is one of testing for a completely known target in noise of known statistics

$$H_0 : \quad X_R : \quad K(\alpha, 0, \Sigma)$$
$$H_1 : \quad X_R : \quad K(\alpha, m \cdot R(\rho)P(\psi)T_n, \Sigma).$$

The resulting polarimetric likelihood ratio test for K-distributed clutter (PLRTK)

$$\frac{p_{X|H_1}(X|H_1)}{p_{X|H_0}(X|H_0)} \overset{H_1}{\underset{H_0}{\gtrless}} \beta \tag{7}$$

chooses between hypotheses with uncommon means and common covariances. Since m, ρ, and ψ, are typically unknown we estimate them in the ML sense and implement a generalized likelihood ratio test [2]

$$\frac{\max_{m,\rho,\psi} p(X|m, \rho, \psi)}{p_{X|H_0}(X|H_0)} \overset{H_1}{\underset{H_0}{\gtrless}} \beta \tag{8}$$

which is simply the standard PLRTK with the unknown quantities replaced by their ML estimates.

7 Preliminary GLRT Results

We begin by looking for closed form expressions for the ML estimates of m, ρ, and ψ. The real form (2) of the measurement vector is distributed as $X : K(\alpha, m \cdot R(\rho)P(\psi)T_n, \Sigma)$. The likelihood function under H_1 is of the form

$$p(X|m, \rho, \psi) = \tag{9}$$
$$q_1 \|X - mD\|_\Sigma^{q_2} K_{q_3}(q_4 \|X - mD\|_\Sigma)$$
$$D \overset{\triangle}{=} R(\rho)P(\psi)T_n$$

where the q_i are non-zero constants independent of m, ρ, and ψ and $\|x\|_\Sigma^2 \overset{\triangle}{=} x^T \Sigma^{-1} x$. To find the ML estimate of m we solve

$$0 = \qquad \frac{\partial p(X|m, \rho, \psi)}{\partial m}$$
$$= \|X - mD\|_\Sigma^{2q_2-2} \left[D^T \Sigma^{-1}(mD - X)\right] f(m) \tag{10}$$

where $f(m)$ is a complicated function of m involving the modified Bessel function K. The first term of (10) is zero only with probability zero. The second term is zero for

$$m = D^T \Sigma^{-1} X / \|D\|_\Sigma^2. \tag{11}$$

This expression for m involves the projection of the whitened measurement vector $\Sigma^{-1/2} X$ onto the whitened target $\Sigma^{-1/2} D$. Given values for ρ and ψ, we see that D is determined and m may be computed from (11). Thus, we need to search only over ρ and ψ for a local extremum of the likelihood function. In fact, the two-dimensional search is bounded since $\rho \in [-\pi/2, \pi/2]$, $\psi \in [0, \pi]$. There does not exist a value of m for which $f(m)$, the third term of (10), is identically zero. Hence, the two-dimensional search procedure described above in fact yields the global ML estimates of m, ρ, and ψ.

422

Next we test the ability of the ML search procedure described above to produce accurate estimates of the true target amplitude, phase, and orientation. To each of 50 clutter pixels $\{C_i, i = 1, \ldots, 50\}$ taken from the polarimetric clutter images we added a linear dipole of amplitude $m = 0.0104$, phase $\rho = 90^\circ$, and orientation $\psi = 0^\circ$ to produce $\{Y_i, i = 1, \ldots, 50\}$ given by

$$Y_i = C_i + 0.0104 \cdot R(90^\circ)P(0^\circ)T_n$$
$$T_n = [\ 1 \ \ 0 \ \ 0 \ \ 0 \ \ 0 \ \ 0 \ ]^T.$$

For each of the Y_i, we computed the ML estimates of m, ρ, and ψ using the two-dimensional search procedure described above. The search was carried out in 5° increments of ρ and ψ. We then repeated the same experiment except that this time we set the dipole orientation to $\psi = 90^\circ$.

Figure 4 shows the ML estimates of m, ρ, and ψ for the two experiments plotted against their true values. In addition, the figure shows the target-to-clutter ratio $t/c = 20\log(\|0.0104 \cdot R(90^\circ)P(0^\circ)T_n\|/\|C_i\|)$ in dB. When ψ was estimated to be 175° in (c), we plotted it as -5°. Figure 4 shows that the experiment with a target orientation of $\psi = 90^\circ$ produced qualitatively (and quantitatively, as measured by standard deviation) better ML estimates of target amplitude m and phase ρ than did the experiment with $\psi = 0^\circ$. This is explained by noting that the clutter histogram of ψ (see Figure 3(c)) is concentrated around 0° and is relatively small at $\psi = 90^\circ$. As expected, the ML estimates improve when the target-to-clutter ratio is large.

8 Conclusions

The goal of this work is to develop methods for detecting scattering center targets in clutter using ultra-wideband fully-polarimetric SAR data. First, we analyzed the statistics of forest clutter and found that the K-distribution provides a better model of the clutter than does the Gaussian distribution. In addition, histograms of the Huynen parameters of the forest clutter are provided to characterize the scattering mechanisms present in the forest and hence to lend insight into the types of man-made scattering centers that are more easily distinguished from clutter with an appropriate detector. Next, we presented a new approach to polarimetric scattering center detection that leads to a generalized likelihood ratio test for scattering center detection in K-distributed clutter (PGLRTK). This test provides detection capability in the presence of unknown target amplitude, absolute phase, and orientation about the line-of-sight. This polarimetric GLRT approach is applicable to other clutter types.

Further work is needed to assess the performance of the proposed PGLRTK relative to that of currently available detectors.

References

[1] R. M. Lewitt, "Reconstruction alogorithms: Transform methods," *Proceedings of the IEEE*, vol. 71, pp. 390–408, March 1983.

[2] H. L. V. Trees, *Detection, Estimation, and Modulation Theory: Part I.* New York: Wiley, 1968.

[3] L. L. Scharf, *Statistical Signal Processing.* Reading, Massachusetts: Addison-Wesley, 1991.

[4] J. R. Huynen, *Phenomenological Theory of Radar Targets.* PhD thesis, Technical University, Delft, The Netherlands, 1970.

[5] A. P. Agrawal and W.-M. Boerner, "On the concept of optimal polarizations in radar meteorology," in *Proceedings of the Polarimetric Technology Workshop*, vol. I.2, (Redstone Arsenal, Alabama), pp. 179–243, August 16–18 1988.

[6] S. H. Yueh, J. A. Kong, J. K. Jao, R. T. Shin, H. A. Zebker, T. L. Toan, and H. Ottl, "Chapter 4: K-distribution and polarimetric terrain radar clutter," in *PIER-3: Progress in Electromagnetics Research: Polarimetric Remote Sensing* (J. A. Kong, ed.), New York: Elsevier, 1990.

[7] L. M. Novak, M. C. Burl, R. D. Chaney, and G. J. Owirka, "Optimal processing of polarimetrc synthetic-aperture radar imagery," *The Lincoln Laboratory Journal*, vol. 3, pp. 273–290, summer 1990.

[8] L. M. Novak, M. B. Sechtin, and M. J. Cardullo, "Studies of target detection algorithms that use polarimetric radar data," *IEEE Transactions on Aerospace and Electronic Systems*, vol. AES-25, pp. 150–165, March 1989.

[9] "Detection in non-gaussian clutter," in *Automatic Detection and Radar Data Processing* (D. C. Schleher, ed.), Dedham, MA: Artech House, Inc., 1980.

[10] E. Jakeman, "On the statistics of K-distributed noise," *J. Phys. A: Math. Gen.*, vol. 13, pp. 31–48, 1980.

[11] L. M. Novak and M. C. Burl, "Optimal speckle reduction in polarimetric SAR imagery," *IEEE Transactions on Aerospace and Electronic Systems*, vol. AES-26, pp. 293–305, March 1990.
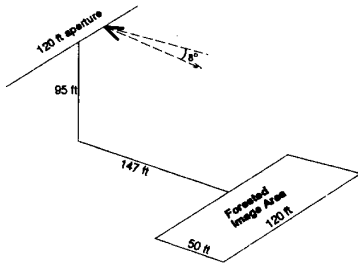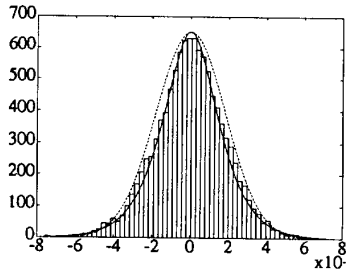
Figure 1. Radar geometry

Figure 2. Pdfs and histogram of real(HH). Solid: K-distribution, Dashed: Gaussian

(a) amplitude m

(a) amplitude m

(b) characteristic angle γ

(b) absolute phase ρ

(c) orientation ψ

(d) ellipticity τ

(c) orientation ψ

(e) skip angle ν
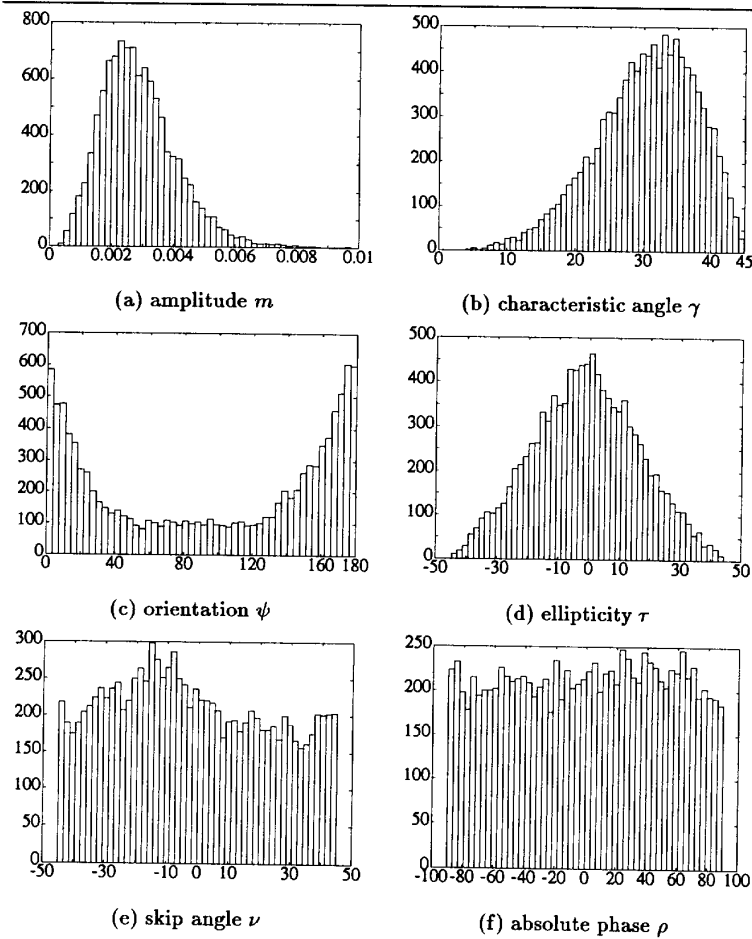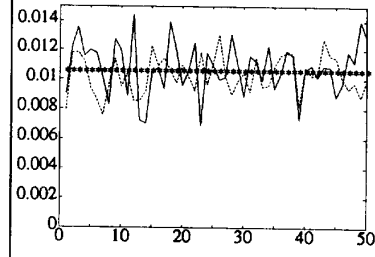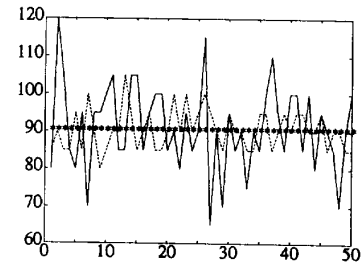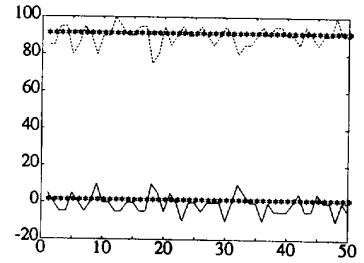
(f) absolute phase ρ

(d) t/c

Figure 3. Histograms of clutter Huynen parameters. Y-axes give # of pixels, X-axes of (b) - (f) are in degrees.

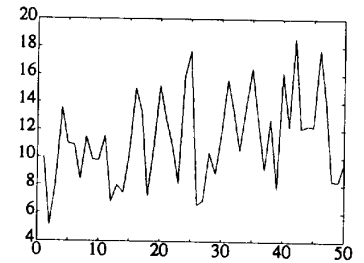Figure 4. (a)-(c) ML estimates and true values of unknowns for the 50 trials. (d) t/c in dB. *: true value, solid: $\psi = 0°$ trials, dashed: $\psi = 90°$ trials.

424